

PAPER

High- m kink/tearing modes in cylindrical geometry

To cite this article: J W Connor *et al* 2014 *Plasma Phys. Control. Fusion* **56** 125006

View the [article online](#) for updates and enhancements.

Related content

- [A current-driven electromagnetic mode in sheared and toroidal configurations](#)
István Pusztai, Peter J Catto, Felix I Parra *et al*.
- [Using a local gyrokinetic code to study global ion temperature gradient modes in tokamaks](#)
P A Abdoul, D Dickinson, C M Roach *et al*.
- [Energetic particle physics in fusion research in preparation for burning plasma experiments](#)
N.N. Gorelenkov, S.D. Pinches and K. Toi

Recent citations

- [Trapped fast particle destabilization of internal kink mode for the locally flattened q-profile with an inflection point](#)
Xian-Qu Wang *et al*
- [Corrigendum: A current driven electromagnetic mode in sheared and toroidal configurations \(2014 *Plasma Phys. Control. Fusion* 56 035011\)](#)
István Pusztai *et al*



IOP | ebooks™

Bringing you innovative digital publishing with leading voices to create your essential collection of books in STEM research.

Start exploring the collection - download the first chapter of every title for free.

High- m kink/tearing modes in cylindrical geometry

J W Connor^{1,2,3}, R J Hastie^{1,2}, I Pusztai^{4,5}, P J Catto^{2,4} and M Barnes^{1,2,6}

¹ CCFE, Culham Science Centre, Abingdon, Oxfordshire, OX14 3DB, UK

² Rudolf Peierls Centre for Theoretical Physics, 1 Keble Rd, Oxford, OX1 3NP, UK

³ Imperial College, London, SW7 2BW, UK

⁴ Plasma Science and Fusion Center, MIT, Cambridge, MA 02139, USA

⁵ Applied Physics, Chalmers University of Technology, Göteborg, SE-41296, Sweden

⁶ Department of Physics, University of Texas, Austin, TX 78712, USA

E-mail: Jack.Connor@ccfe.ac.uk

Received 11 July 2014, revised 15 September 2014

Accepted for publication 24 September 2014

Published 29 October 2014

Abstract

The global ideal kink equation, for cylindrical geometry and zero beta, is simplified in the high poloidal mode number limit and used to determine the tearing stability parameter, Δ' . In the presence of a steep monotonic current gradient, Δ' becomes a function of a parameter, σ_0 , characterising the ratio of the maximum current gradient to magnetic shear and x_s , characterising the separation of the resonant surface from the maximum of the current gradient. In equilibria containing a current 'spike', so that there is a non-monotonic current profile, Δ' also depends on two parameters: κ , related to the ratio of the curvature of the current density at its maximum to the magnetic shear and x_s , which now represents the separation of the resonance from the point of maximum current density. The relation of our results to earlier studies of tearing modes and to recent gyrokinetic calculations of current driven instabilities, is discussed, together with potential implications for the stability of the tokamak pedestal.

Keywords: tearing mode, radially global, magnetohydrodynamic stability, gyrokinetic simulation

(Some figures may appear in colour only in the online journal)

1. Introduction

Most studies of micro-instabilities consider those driven by gradients of density or ion and electron temperatures. However the toroidal current gradient is also a potential source of instability. Indeed, this is the instability drive for tearing modes and it was even proposed [1] that it could drive high mode number ideal magnetohydrodynamic (MHD) kink instability. This analysis was based on the periodic, cylindrical, ideal MHD equation for the perturbed magnetic flux function, $\Psi = \psi(r) \exp[i(m\theta - nz/R)]$, in the tokamak limit, $B_\theta/B_z \sim r/R \ll 1$:

$$\frac{d}{dr} r \frac{d\psi}{dr} - \frac{m^2}{r} \psi - \frac{\hat{J}'}{1/q - n/m} \psi = 0, \quad (1)$$

where r ($0 < r < a$) is the radial coordinate with $'$ denoting a radial derivative, θ the azimuthal angle and z the axial

co-ordinate, $2\pi R$ being the periodicity length in the z -direction and we have introduced 'poloidal' and 'toroidal' mode numbers, m and n , respectively. The magnetic field in the z -direction is B_0 , the safety factor $q = rB_0/R B_\theta$ and the normalised current density, \hat{J} , is defined by

$$\hat{J}(r) = \frac{4\pi R J(r)}{c B_0}. \quad (2)$$

Expanding the denominator of (1), $(1/q - n/m)$, in the vicinity of the resonant position, r_s , where, $m - nq(r_s) = 0$, so that

$$\frac{1}{q} - \frac{n}{m} \simeq -\frac{sx}{mq}, \quad (3)$$

with

$$x = m(r - r_s)/r_s, \quad (4)$$

denoting a new (dimensionless) local radial variable, this equation takes the local form:

$$\frac{d^2\psi}{dx^2} - \left(1 + \frac{\sigma_0}{x}\right)\psi = 0, \quad (5)$$

where

$$\sigma_0 = -\frac{r_s \hat{J}'}{ns}, \quad (6)$$

with $s = rq'/q$ being the magnetic shear at $r = r_s$. Equation (5) has been the basis for a number of studies at high m . Thus Kadomtsev and Pogutse [1] used it to claim that ideal MHD instability is possible, for steep current gradients or low shear, if

$$\sigma_0 > 2, \quad (7)$$

while Wesson [2] and Strauss [3] investigated the dependence of the tearing mode index, Δ' [4] on σ_0 . Hegna and Callen [5] used a generalisation of (5) that took account of the effect of toroidal and plasma shaping on metric coefficients, to estimate Δ' in more general, toroidal, devices. Furthermore, the local gyrokinetic code GS2 has recently [6] been used to study current gradient driven instabilities in collisionless plasmas, again finding instability above a critical value of σ_0 . However this code is based on the ballooning transformation and this also relies on a linear expansion of q about the rational surface.

Unfortunately such treatments are not entirely consistent because, for $\sigma_0 \sim \mathcal{O}(1)$, the truncated expansion of $(q - m/n)$ employed is inadequate. To see this is the case recall $\hat{J}(r)$ and $q(r)$ are related through Ampère's equation,

$$\hat{J} = \frac{1}{r} \frac{d}{dr} \left(\frac{r^2}{q} \right), \quad (8)$$

which can be written $\hat{J} = (2 - s)/q$, so that

$$r\hat{J}' = (2s^2 - 3s - w)/q, \quad (9)$$

with w denoting the quantity $r^2 q''/q$. Now if we restrict attention to positive values of the current density, $\hat{J}(r)$, then $s < 2$ and $|2s^2 - 3s| \sim \mathcal{O}(1)$. The condition $|r\hat{J}'| \gg 1$ then implies $|w| \gg 1$ so that terms in q'' must be retained in the expansion of q around r_s , giving $\sigma_0 = w/(ms)$. Consequently, if the parameter σ_0 is of order unity, as in [1–3], the tearing equation must now take the form:

$$\frac{d^2\psi}{dx^2} - \left[1 + \frac{\sigma_0}{x(1 + \sigma_0 x/2)}\right]\psi = 0. \quad (10)$$

Equation (10), however, of necessity describes a scenario in which there are two resonant surfaces; a situation which cannot be the case for a monotonic $q(r)$ even when $\sigma_0 \sim \mathcal{O}(1)$. We conclude that both (5) and (10) must give a flawed description of stability of monotonic $q(r)$ profiles. Clearly, higher order terms in the expansion of $q - n/m$ are required. Thus, remarkably, there is no truly local theory for such high- m instabilities. We note that a comparison of analytic resistive tearing mode growth rates with those obtained from a numerical code at low- m also required the inclusion of more derivatives of $q(r)$ to obtain agreement when the resistivity and Δ' were relatively high [7].

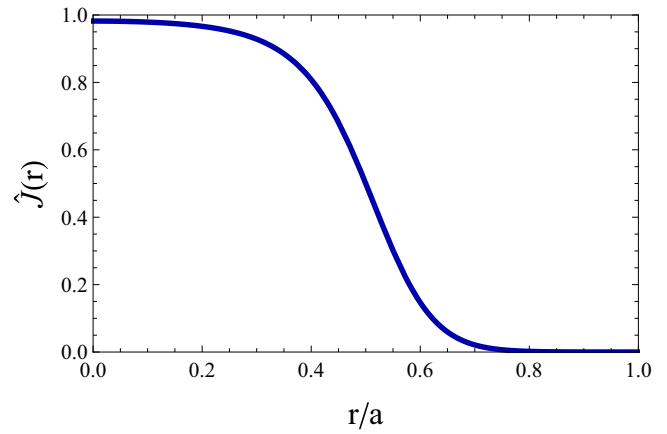


Figure 1. $\hat{J}(r)$ of (11), with $J_0 = 1$, $\lambda = 4$ and $r_0/a = 0.5$.

In this paper we reconsider the solution of (1) at high m , taking full account of the structure of $\hat{J}(r)$ and $q(r)$. Two scenarios are studied: (i) a monotonic $\hat{J}(r)$ with a steep gradient, modelled by a ‘tanh function’; and (ii) the effect of a positive current ‘spike’, possibly arising in the pedestal region of a tokamak in H-mode due to bootstrap currents. This latter case can lead to a region of greatly reduced shear, or even non-monotonic $q(r)$ and multiple resonances. The outcomes of our calculations are self-consistent forms for Δ' which can be used to investigate high- m tearing mode instability. A value of Δ' that accounts for key nonlocal features of the global structure of the self-consistent q and current profiles is required to properly interpret the GS2 results alluded to above. The quantity Δ' also plays a role in determining the saturated amplitude of magnetic islands arising from tearing mode instability. However other parameters may play a role in determining this amplitude [8].

2. Reduction of the tearing equation for high- m : monotonic current profiles

In this section we consider a specific example for the current density $\hat{J}(r)$ which has a steep gradient and exploit the property $m \gg 1$ to expand (1) close to the resonant surface at r_s . The current density employed is

$$\hat{J}(r) = \frac{J_0}{2} \left\{ 1 - \frac{\tanh[\lambda(r^2 - r_0^2)/(2r_0^2)]}{\tanh[\lambda(a^2 - r_0^2)/(2r_0^2)]} \right\}, \quad (11)$$

where r_0 is the point of steepest current gradient and we will be interested in large values of the parameter $\lambda \sim \mathcal{O}(m)$. The current profile of (11) is shown in figure 1 for $J_0 = 1$, $\lambda = 4$ and $r_0/a = 0.5$. Integrating the Ampère equation, (8), yields an expression for the resonant denominator in the tearing equation, (1), viz.:

$$\begin{aligned} \frac{1}{q(r)} - \frac{n}{m} &= \frac{J_0 r_0^2}{2\lambda t} \left\{ \frac{1}{r_s^2} \log \left[\cosh \frac{\lambda(r_s^2 - r_0^2)}{2r_0^2} \right] \right. \\ &\quad \left. - \frac{1}{r^2} \log \left[\cosh \frac{\lambda(r^2 - r_0^2)}{2r_0^2} \right] + \log \left(\cosh \frac{\lambda}{2} \right) \left(\frac{1}{r^2} - \frac{1}{r_s^2} \right) \right\}, \\ t &\equiv \tanh \left[\frac{\lambda}{2r_0^2} (a^2 - r_0^2) \right], \end{aligned} \quad (12)$$

where r_s denotes the location of the resonance, i.e.

$$q(r_s) = \frac{m}{n}. \quad (13)$$

The numerator of the resonant term in (1) is readily evaluated to give

$$r\hat{J}' = -\frac{J_0\lambda r^2}{2tr_0^2} \operatorname{sech}^2\left[\frac{\lambda}{2r_0^2}(r^2 - r_0^2)\right]. \quad (14)$$

We next introduce the local radial variable $x = m(r - r_0)/r_0$, where we have now chosen r_0 rather than r_s as origin and corresponding resonance position, $x_s = m(r_s - r_0)/r_0$ and express $\hat{J}(x)$ and $q(x)$ as functions of x around $r = r_0$, noting that these expressions are not confined to small values of x , since we only require $|x/m| \ll 1$. Therefore, using $t = 1$ and ignoring $\mathcal{O}(1/m^2)$ corrections in $(r_s/r_0)^2 = 1 + (2x_s/m)$, we find

$$\hat{J}(x) = \frac{J_0}{2} [1 - \tanh(px)], \quad (15)$$

$$\frac{1}{q(x)} - \frac{1}{q(x_s)} = -\frac{J_0}{2\lambda} \{p(x - x_s) + \log[\cosh(px)] - \log[\cosh(px_s)]\}, \quad (16)$$

$$r\hat{J}' = -\frac{\lambda J_0}{2} \operatorname{sech}^2(px), \quad (17)$$

$$p \equiv \frac{\lambda}{m}, \quad (18)$$

where integrating (8) from $r = 0$ to r_0 gives $J_0q(r_0) = 2 + \mathcal{O}(1/\lambda)$ for $\lambda \sim m \gg 1$. When $x_s = 0$, we may write the kink/tearing equation in the form of (5), with

$$\sigma_0 \rightarrow \sigma(x) \equiv \frac{p^2 x \operatorname{sech}^2(px)}{px + \log[\cosh(px)]}. \quad (19)$$

Since we can identify $p = \sigma(0)$, there is again a single parameter, $\sigma(0)$, determining stability, with

$$\sigma(x) = \sigma(0) f[\sigma(0)x], f(y) = \frac{y \operatorname{sech}^2(y)}{y + \log[\cosh(y)]}. \quad (20)$$

Thus we can consider (19) as a semi-localised generalisation of (6) in which σ_0 acquires a form factor, f . The function $\sigma(x)$ is shown in figure 2 for $\sigma(0) = 1$, from which it is clear that $\sigma(x)$ is very far from being constant, as assumed in the local treatments of [1] and [2].

Furthermore, if we assume that the mode numbers, m and n are such that the resonant surface lies at $x = x_s$, i.e. that $m/n = q(x_s)$ rather than $m/n = q(0)$, the tearing equation can be written in what we will refer to as the semi-local form:

$$\frac{d^2\psi}{dx^2} - \psi \left\{ 1 + \frac{p^2 \operatorname{sech}^2(px)}{p(x - x_s) + \log[\cosh(px)] - \log[\cosh(px_s)]} \right\} = 0, \quad (21)$$

with dependence on two parameters, $p \equiv \sigma(0)$ and x_s .

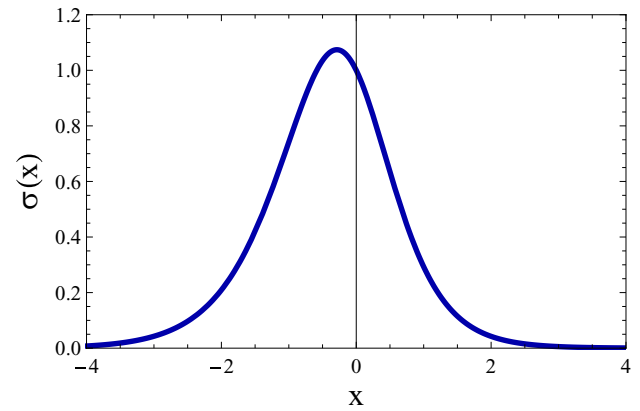


Figure 2. Plot of $\sigma(x)$ for the \hat{J} of figure 1, $p = \sigma(0) = 1$ and $x_s = 0$.

3. Calculation of the tearing mode index, Δ'

In this section we consider reconnecting instabilities which might be driven by the energy source associated with a steep monotonic current gradient, i.e. instabilities which are driven by positive values of the tearing index, Δ' , defined as the jump in ψ'/ψ as in [4]. However we first discuss the ideal MHD stability properties of (21), noting that these can be determined by computing the stability properties of the two Newcomb [9] sub-intervals, $[0, r_s]$ and $[r_s, a]$, or, in terms of the 'local' variable, x , $[-\infty, x_s]$ and $[x_s, +\infty]$. This analysis has been carried out numerically and no instability found at any finite values of the parameters p and x_s (i.e. in Newcomb terms, in shooting a solution which is regular at one end-point of a sub-interval, no zero of $\psi(r)$ is encountered before the other end of the sub-interval is reached). In particular, the value $p = \sigma(0) = 2$ is NOT a marginal point for ideal MHD instability, contrary to [1].

Returning to the issue of tearing mode stability, we calculate $\Delta(p, x_s)$, defined as the jump in $\psi'(x)/\psi(x)$ at x_s for the solution of (21) which vanishes at $x \rightarrow -\infty$ and at $x \rightarrow +\infty$. The global value of Δ' is then related to Δ by:

$$r_s \Delta' = m \Delta. \quad (22)$$

Figure 3 shows Δ as a function of p when $x_s = 0$ and figure 4 shows Δ as a function of x_s for $p = 1$ (solid line) and $p = 0.67$ (dashed line). The somewhat surprising content of figure 4, namely that the most unstable location for the resonant surface is at large negative values of x_s , is an artefact of our semi-local approximation, as discussed below.

We have also performed global calculations of $\Delta = [r_s \Delta'(r_s)]/m$, with $\hat{J}(r)$ given by (11). The results of such global calculations are shown in figure 5 where, for the purpose of comparing with figure 4, (22) has been used to transform 'global' data into 'local' variables, as in figure 4. In figure 5 the parameters are $r_0/a = 0.5$ and $\lambda = m = 8$ (solid curve) and $\lambda = m = 12$, (dashed curve). Figure 5 shows that the most unstable value of Δ occurs at a finite negative value of x_s . A more careful inspection of the derivation of (21) reveals that, at large negative values of x_s , the shear, $s(x_s)$, becomes exponentially small, $\sim \exp(-p x_s)$, so that terms of order $1/m$, which have been neglected, can compete, leading to the behaviour

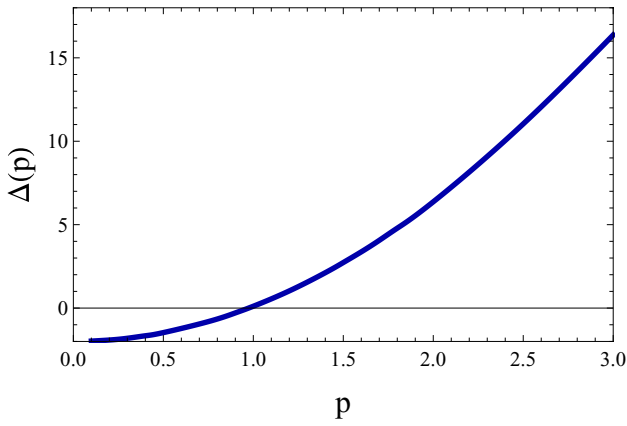


Figure 3. $\Delta(p)$, for $x_s = 0$ as a function of $p = \sigma(0)$ calculated from (21). The transition to unstable tearing occurs at $p \approx 0.97$.

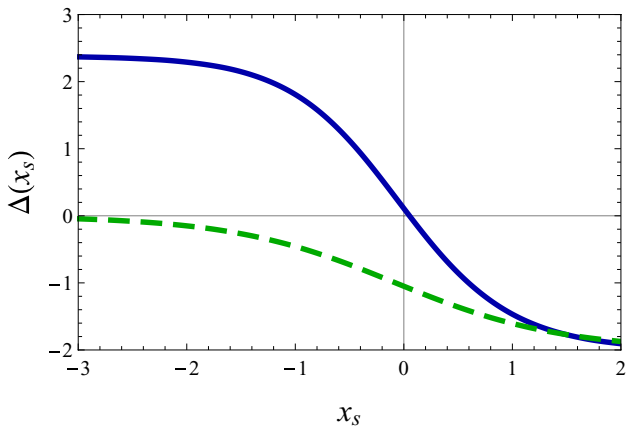


Figure 4. Plot of $\Delta(x_s)$, calculated from (21) for $p = 1$ (solid curve) and $p = 0.67$ (dashed curve).

seen in figure 5, for large, but finite, m . Not surprisingly, the Δ' values obtained and therefore stability, are sensitive to the global structure of the ideal MHD region since equation (21) contains less global information than equation (11), thereby resulting in the differences in Δ shown in figures 4 and 5.

4. Comparison with previous studies

For comparison with the previous results of Kadomtsev and Pogutse [1] and Wesson [2], we have also calculated the tearing stability index $\Delta_0(p)$ obtained by computing solutions of (5) with $\sigma_0 = p$.

Figure 6 shows (dashed curve) the resulting $\Delta_0(p)$ as a function of p from (5). For comparison the solid line shows $\Delta(p)$ of figure 3, computed with $\sigma = \sigma(x)$ of (19). Ideal MHD marginality, where the value of $\Delta_0(p)$ becomes infinite, apparently occurs at $p = 2$ which corresponds to the prediction [1] of ideal kink instability beyond this value. At the value $p = 2$, an exact solution of (5) in the inner Newcomb sub-interval is $\psi = x e^x$, which vanishes at both end-points, again demonstrating ideal marginality. However, as noted in the foregoing discussion, this is an incorrect prediction and is not found in full cylindrical solutions, or in our semi-localised version (19) with the correct $\sigma(x)$ dependence, which yields the solid curve

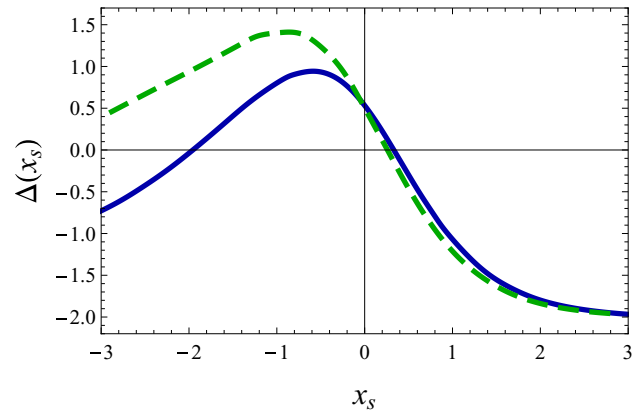


Figure 5. Plot of $\Delta(x_s)$ as a function of x_s , similar to figure 4 but calculated from solution of the global kink/tearing equation (1), with $\hat{J}(r)$ given by (11). $r_0/a = 0.5$ and $m = \lambda = 8$ (solid curve) and $\lambda = m = 12$, (dashed curve), parameters which correspond to $p = 1$ in the local approximation. As described in the text, (22) has been used to present the results in terms of the ‘local’ variables, Δ and x_s .

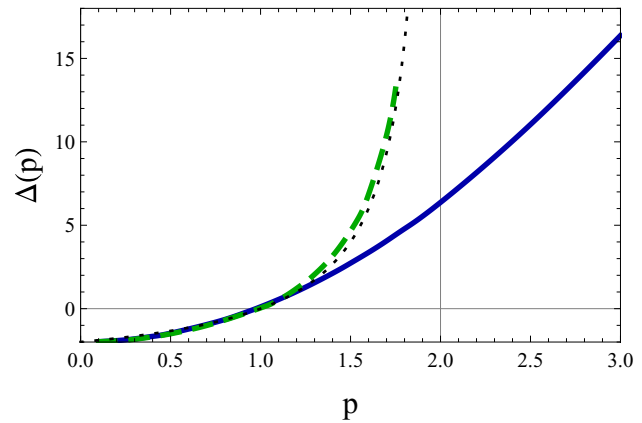


Figure 6. Comparison of Δ_0 with figure 3. The solid curve was computed with $\sigma(x)$ given by (19), the dashed curve was computed with constant $\sigma = p$. Δ_0 passes through zero at $p = 1$, as found in [2] and asymptotes to ∞ at $p = 2$ as in [1]. The thin dotted curve represents a rational approximation to the dashed curve, used in section 5.

in figure 6. For small values of p , Δ_0 is negative and changes sign at $p \approx 1$, as reported in [2].

5. Reduction of the tearing equation for high- m : non-monotonic current profiles

In this section we investigate a different, but possibly important, scenario in which a fairly localised positive current spike occurs relatively near the plasma edge [10, 11], where resistivity is high and the inductive current density is small. The non-linear theory of external kink modes in the presence of such a current spike has been studied by Eriksson and Wahlberg [12]. Bootstrap currents in the region of a steep pedestal, or localized current drive, may produce just such a situation. Figure 7 shows an example for the current density given by,

$$\begin{aligned} \hat{J}(r) &= \hat{J}_0(r) + \hat{J}_1(r), \\ &= J_0[1 - (r/a)^2]^3 + J_1 e^{-\mu(r/r_1-1)^2}, \end{aligned} \quad (23)$$

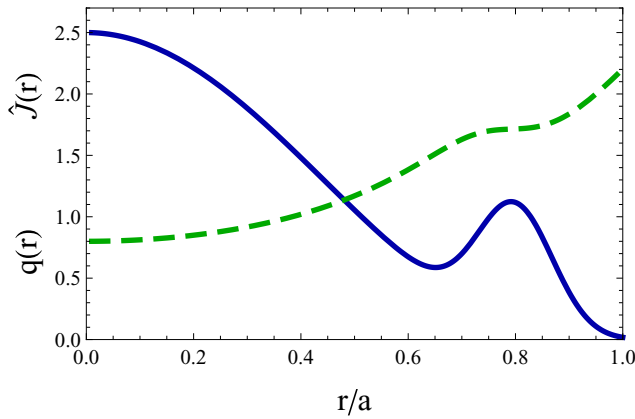


Figure 7. Example of the non-monotonic class of current profile investigated in section 5. The dashed curve shows the $q(r)$ profile displaying reduced magnetic shear in the vicinity of the current spike, $J_1(r)$. Parameters are $J_0 = 2.5$, $J_1 = 1$, $\mu = 64$ and $r_1/a = 0.8$.

with $J_0 = 2.5$, $J_1 = 1$, $\mu = 64$ and the peak of the current spike at $r_1/a = 0.8$. In figure 7 the dashed curve represents the resulting safety factor, $q(r)$, indicating that the magnetic shear becomes small in the region of the current spike.

It might be thought that the most unstable location for a tearing mode resonance would be at the minimum of the current density ($r/a = 0.65$ in figure 7), since the gradient of the current density is destabilising on both sides of the resonance in this case, that is, $J' / [(1/q) - 1/q(r_s)] < 0$ so its sign is the opposite of the stabilizing m^2 line bending term in (1). Surprisingly, however, this is not the case, as can be seen from figure 8 which displays the value of $r_s \Delta'(r_s)$ for an $m = 4$ mode, calculated from (1), as r_s is moved across the $\hat{J}(r)$ profile, regarding n as a continuous variable.

Figure 8 does show that when r_s is located at the maximum of the current spike, $r_s/a \approx 0.79$ in figure 7, the tearing index, Δ' is strongly stabilising (i.e. negative) as one would expect since the current gradients on both sides of r_s are stabilising in this case, that is, $J' / [(1/q) - 1/q(r_s)] > 0$, enhancing the stabilizing m^2 line bending term in (1). However, values of r_s quite close to the maximum of the current spike are very unstable.

To model this in a high- m , localised analysis, we expand $\hat{J}(r)$ and $q(r)$ locally around the maximum of the current density, approximately at r_1 , the maximum of the current spike. Around this point, $\hat{J}(r)$ is dominated by the current spike, $\hat{J}_1(r)$ and is a local function, $\hat{J}_1(x)$, if we order the parameter $\mu \sim \mathcal{O}(m)$. However, the q profile in this region is determined by both the extended ‘inductive’ current profile $\hat{J}_0(r)$ and by the current spike. It therefore contains both a slowly varying part, due to $\hat{J}_0(r)$ and a rapidly varying part, due to $\hat{J}_1(r)$ and the result can be a greatly reduced magnetic shear, as seen in figure 7. The resulting local tearing equation has been derived in the appendix A, for the current profile of (23). However a simpler derivation expands $q(r)$ locally around the point, r_1 , at the maximum of $\hat{J}(r)$ and orders the weakened shear, $s \sim 1/m$ and $r_1^3 q''' / q \sim m \gg 1$. Thus:

$$q(x) = q(r_1) + r_1 q' \frac{x}{m} + \frac{1}{6} r_1^3 q''' \frac{x^3}{m^3}. \quad (24)$$

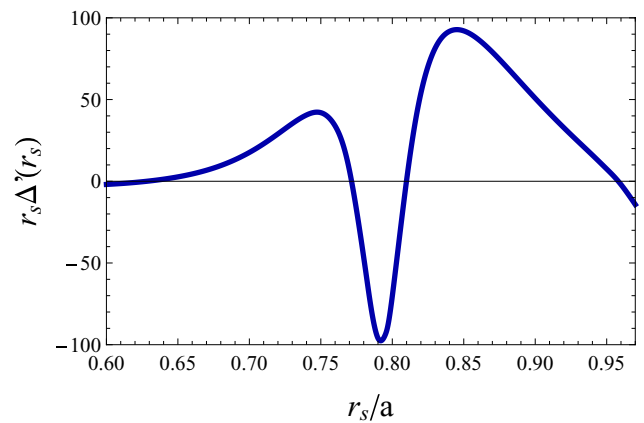


Figure 8. Plot of $r_s \Delta'(r_s)$ for an $m = 4$ mode, from solution of (1) with $\hat{J}(r)$ given by (23).

Then, constructing $\hat{J}'(x)$ from (23), the high- m tearing mode equation (1), can be written in the form;

$$\frac{d^2 \psi}{dx^2} = \psi \left[1 + \frac{\kappa x}{x(1 + \frac{1}{6} \kappa x^2) - x_s(1 + \frac{1}{6} \kappa x_s^2)} \right], \quad (25)$$

$$\kappa = \frac{r_1^3 q'''}{m^2 r_1 q'},$$

where x_s is again the location of the resonance. We note from (24) that a monotonic q profile requires $\kappa > 0$.

As in section 3, stability depends on two parameters, κ and x_s . In order to reduce the parameter space in (25), we have focused on three cases:

$$(a) \kappa = 8 \quad \text{monotonically increasing } q, \quad (26)$$

$$(b) \kappa = 64 \quad \text{with weaker shear at } x = x_s, \quad (27)$$

$$(c) \kappa = -8 \quad \text{non-monotonic } q(r). \quad (28)$$

Equation (25) has then been solved to obtain values of $\Delta(x_s)$ as the resonant location, x_s , is moved across the local $q(x)$ structure. Results for cases (a) and (b), equations (26) and (27) respectively, are shown in figure 9. The solid curve corresponds to case (a) and the dashed one to case (b). In case (c), (28), we exclude consideration of the region of triple resonance, i.e. $-1 < x_s < +1$ and figure 10 shows the value of Δ when x_s falls outside this range. Consideration of the triple resonances in case (c) raises issues involving the different characteristic frequencies associated with tearing at each of the three resonant surfaces, these frequencies being determined by diamagnetic terms and by sheared equilibrium rotation. In addition, case (c) is likely to arise only after an equilibrium current profile has evolved through the very unstable weak shear scenario, case (b). It is therefore sufficient to note that as x_s approaches the location of q_{\min} or q_{\max} , the value of Δ becomes very large.

Positive values of Δ , with energy available to drive reconnection, are predicted for modes which are resonant close to, but not at, the local maximum of the current density. Comparison of figures 8 and 9 demonstrates the validity of the high- m equation (25).

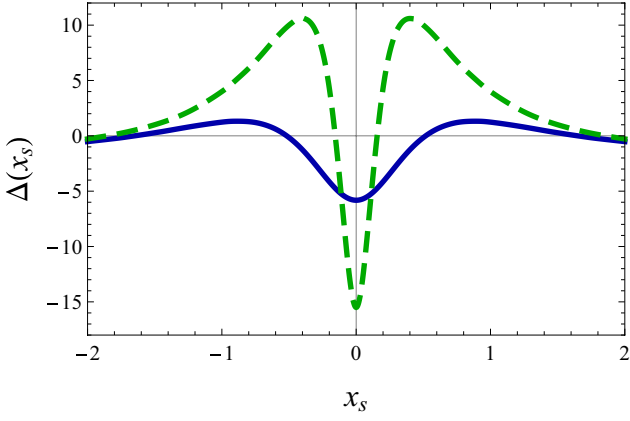


Figure 9. Plot of $\Delta(x_s)$, from (22) with $\kappa = +8$ (solid curve) and $\kappa = 64$ (dashed curve), corresponding to monotonically increasing q profiles.

6. GS2 Results

GS2 is a radially local gyrokinetic code modeling small scale instabilities ($k_y a \gg 1$) in a periodic flux-tube domain in toroidal geometry. Here, $k_y = n q_r / r_r$ is the binormal wave number, where n is the toroidal mode number and the subscript r of a quantity refers to its value at the reference radius. The radial variation of the metric is not retained and all plasma and magnetic geometry parameters are linearized around their value at r_r . In particular, $q \approx q_r [1 + s_r (r - r_r) / r_r]$ is used: an approximation equivalent to (3). For brevity, henceforth we will drop the r subscripts. We use the low-flow version of GS2 [13], similarly as described in [6] and model the current as a parallel velocity shift in the non-fluctuating Maxwellian electron distribution. We consider a collisionless, pure deuterium plasma where both species are gyrokinetic. We use a large aspect ratio, circular cross section geometry with no finite pressure corrections to the flux surfaces and we neglect compressional magnetic perturbations.

The following parameters are used for the simulations: $u/v_i = 1$, $\beta_i = 0.01$, $a/L_u = 3$, $a/L_{Ti} = a/L_{Te} = a/L_n = 0$, $k_y \rho_i = 0.15$, $a/R_0 = 0.1$, $r/a = 0.5$, $s = 1$. Here, $-u$ is the electron flow speed, $v_i = (2T_i/m_i)^{1/2}$ is the ion thermal speed with T_i and m_i the temperature and the mass of ions, $\beta_i = 8\pi p_i / B_0^2$ is the normalized ion pressure, $d \ln u / dr = -1/L_u$, $d \ln n_e / dr = -1/L_n$, $d \ln T_e / dr = -1/L_{Te}$ and $d \ln T_i / dr = -1/L_{Ti}$. Furthermore, $\rho_i = v_i / \Omega_i$ is the ion thermal Larmor radius with the gyro-frequency $\Omega_i = e B / m_i c$, R_0 is the major radius at the centroid of the flux surface. We choose to set the temperature and density gradients to zero, thus there are no diamagnetic corrections to the mode frequency and we can avoid the pollution of the results with pressure gradient driven instabilities. Therefore the current gradient is purely due to a gradient in the electron flow speed.

We scan the safety factor q , which changes the current gradient drive parameter $\sigma = -2L_s \beta_i u (n_e T_i / e) (d \ln J / d\psi_0) / (k_y^2 \rho_i^2 v_i^2)$ through the shear length $L_s = q R_0 / s$. Here, we introduced the unperturbed poloidal flux $2\pi\psi_0$. In cylindrical geometry, this definition of σ is equivalent to σ_0 in (6). When we set all plasma and geometry parameters to their values specified in the previous paragraph and let q vary, we find $\sigma = 2q$. For the

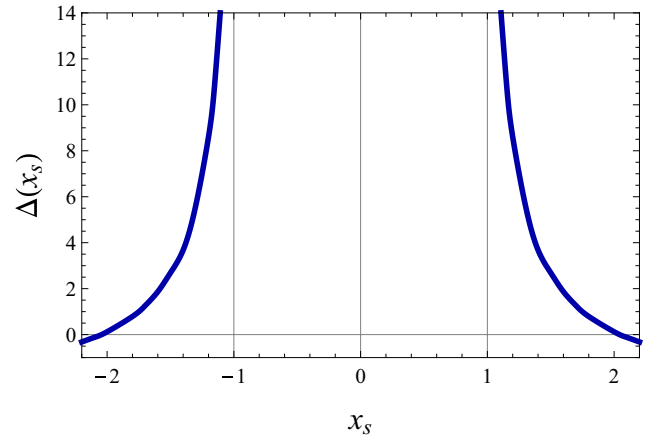


Figure 10. Equivalent plot to figure 9 but with $\kappa = -8$ corresponding to reverse shear at $x = 0$, i.e. to a locally non-monotonic q profile. Δ values are only calculated when there is a single resonant surface, i.e. in the range $|x_s| > 1$.

same set of parameters the spurious ideal kink instabilities are found above $\sigma = 2$ ($q = 1$), see figure 2(e) in [6]. Here we will concentrate on the region $1 < \sigma < 2$, where destabilization of current-gradient driven tearing modes is possible ($\Delta > 0$), as indicated by the dashed line in figure 6.

Figure 11(a) shows the growth rate of the tearing mode as a function of p ($\equiv \sigma$). The symbols represent the GS2 simulation results. The real part of the frequency (not shown here) is very small in magnitude, consistent with being zero within the numerical accuracy of the calculations. We did not perform simulations below $p = 1.5$ since the decreasing growth rates lead to unreasonably long simulation times to reach convergence. The simulations barely resolve the collisionless electron skin depth by covering an unusually large range of ballooning angles; the number of 2π segments along the field line is 40 in the simulations (we note that convergence of the results with respect to resolution has been checked).

The growth rate of the collisionless tearing mode, within a constant, is given by $\gamma \simeq \Delta_k k_y v_e / L_s$ [14], where $\Delta_k = \Delta' \delta_e^2$ is the width of the inner layer, with $\delta_e^2 = c^2 / \omega_{pe}^2 = (m_e / m_i) \rho_i^2 / \beta_i$, ω_{pe} is the electron plasma frequency, $v_e = (2T_e / m_e)^{1/2}$ is the electron thermal velocity and Δ' is the jump in $d \ln \psi / dr$ across the inner layer. Introducing the dimensionless $\Delta = \Delta' / k_y$, we find that $\gamma [v_i / a] \simeq \Delta (k_y \rho_i)^2 \beta_i^{-1} (s a) / (q R) [(m_e T_e) / (m_i T_i)]^{1/2}$. We may use the following rational approximation to describe the p -dependence of Δ found from local ideal MHD calculations: $\Delta \approx 4(p - 1) / (2 - p)$, shown as the dotted curve in figure 6. The dotted line in figure 11(a) represents the growth rate as estimated by the above expressions for γ and $\Delta(p)$. Approximations in the model break down close to the ideal MHD instability limit, $p = 2$, where the predicted values of γ and Δ_k diverge.

Typical radial mode structures are shown in figure 11(b); the p values shown here are 1.5625 and 1.9375. Since GS2 solves the problem in ballooning angle θ and not in $x = (r - r_s) k_y$, the plotted functions are obtained from the appropriate Fourier transform of the parallel component of the perturbed vector potential. The eigenfunctions ψ are normalized so that their value is 1 at the maximum of $|\psi|$ appearing close to $x = -1$;

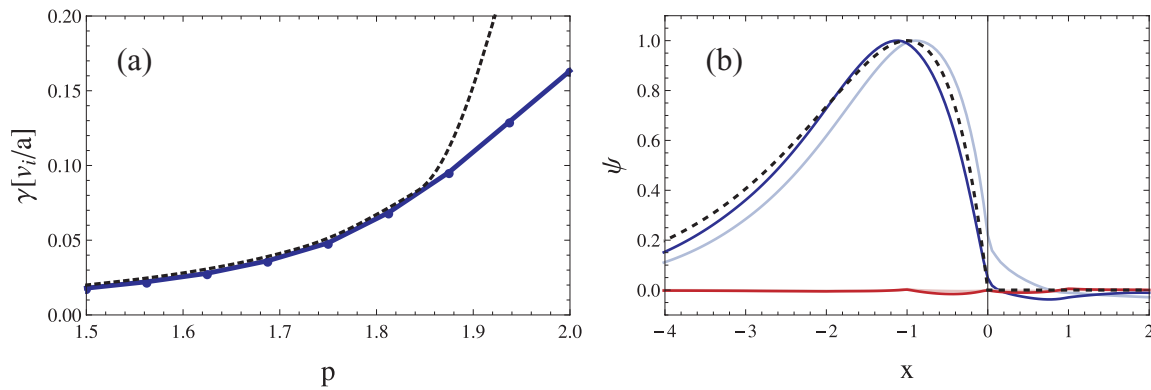


Figure 11. (a) Growth rate of the current driven instability in the p range where the ideal kink mode is stable. Blue curve and symbols denote GS2 results, dotted line represents an analytical estimate based on [14]. (b) Typical radial structures of tearing modes inferred from GS2 simulations. Blue lines: real part, red lines (mostly overlapping, with values close to zero): imaginary part. Dashed line: analytical solution of marginally stable ideal kink. Darker curves: $p = 1.9375$, lighter curves: $p = 1.5625$.

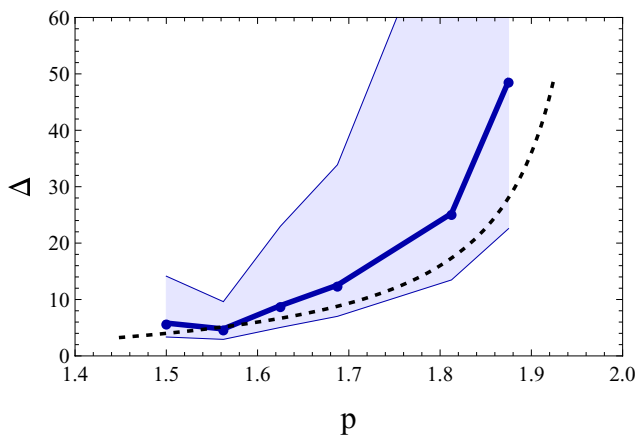


Figure 12. Δ as a function of p . Solid line with circle markers: estimated value from GS2 simulations. Light blue shaded area: Uncertainty in GS2 results. Dashed line: rational approximation of the local ideal MHD result.

then the blue (red) curves represent the real (imaginary) part of ψ . The eigenfunctions do not change appreciably as p is varied. In fact they very much resemble the well known marginally stable ideal MHD result which is of the form xe^x for $x < 0$ and 0 for $x > 0$ (indicated with black dotted curve in the figure).

Taking these $\psi(x)$ eigenfunctions, we can estimate Δ from the GS2 simulations. As also seen in figure 11(b), the eigenfunctions are affected by numerical error. In the calculation of Δ' a division by $\psi(0)$ needs to be made, which amplifies small errors as $\psi(0)$ approaches 0, which happens close to the spurious ideal stability limit $p = 2$. Therefore, we are unable to determine Δ quantitatively. Figure 12 shows the estimated values of Δ from GS2 simulations for a range of p values (circle symbols and solid curve). The confidence intervals of the results are indicated with the shaded area, obtained by perturbing the eigenfunction within numerical uncertainties. As p approaches 2, the uncertainties diverge; accordingly, we do not show values of Δ above $p = 1.875$. As a reference, we show the rational approximation of the ideal MHD result by the dotted line (this is the same as the dotted curve of figure 6).

7. Summary and conclusions

This investigation was stimulated, in part, by simulation results from GS2 [6], with a possible interpretation of an observed instability as an ideal current driven kink. Such a ‘ballooning space’ calculation assumes the neglect of q'' and all higher derivatives: i.e. it is equivalent to the approximations which lead to (5) in configuration space, an equation which, incorrectly, predicts ideal instability for values of $\sigma_0 > 2$, where σ_0 is related to the ratio of current gradient to magnetic shear. It therefore appears that the ‘ideal’ instability seen in GS2 is spurious. However, the calculations presented here show that the consequence of correctly retaining the full functional dependence of $\sigma(x)$ in, for example, (21), is to exclude the possibility of ideal kink instability, while still permitting unstable values of the tearing index, Δ' , when $\sigma(0)$ exceeds a value around unity. Hence the mode identification in terms of a ‘tearing/kink’ drive looks entirely justified, but its identification as an ‘ideal kink’ as proposed by Kadomtsev and Pogutse [1], should be modified. The mode should be regarded as a high- m tearing mode, driven unstable by a large value of Δ' , with collisionless reconnection provided by electron physics in the resonant layer around r_s . As a consequence, it will be inappropriate to run GS2 with values of $\sigma_0 > 2$. It is also of interest to note that Hegna and Callen [5] used a modification of (5) to describe general geometry and as a simple way to derive a convenient formula for Δ' in toroidal systems. Although this may give a good approximation for values of $\sigma_0 < 1$, where Δ' is negative, it overestimates the instability drive for $\sigma_0 > 1$ and predicts ideal instabilities for $\sigma_0 > 2$, where none exist.

We have also investigated a situation with a non-monotonic profile of the current density, $\hat{J}(r)$, as might result from bootstrap currents near a tokamak pedestal. Stability of high- m modes is again governed by a local equation (25), depending on two parameters, κ and x_s , where κ is a measure of the ratio $r_s^2 q''' / m^2 q'$ and x_s is the location of the resonance relative to the point of maximum J . As for the previous case, ideal instability does not occur for any values of the κ and x_s parameters, but positive values of the tearing index, Δ' can be found for sufficiently large values of κ . Such values of κ can

arise from the low shear resulting from the near cancellation of contributions from the background current and the current spike. These situations can, typically, lead to $\Delta \sim \mathcal{O}(1)$, implying $r_s \Delta' \sim \mathcal{O}(m) \gg 1$. Since such a current spike can result from the bootstrap current occurring naturally in the pedestal region of a tokamak H-mode plasma, these observations have possible relevance for the interpretation of ELMs in terms of surface ‘peeling’ modes associated with tearing modes resonant within the pedestal. They also suggest the possibility of influencing ELM behaviour by driving reverse currents within the pedestal region. We note that the potentially large values of Δ' could overcome stabilising effects, such as the Glasser effect in a torus [15] arising from a pressure gradient at the resonant surface in resistive MHD, or from diamagnetic effects associated with the steep gradients in the pedestal in hotter plasmas [16, 17]. To ameliorate the deleterious effects of large ELMs on divertor target plates, resonant magnetic perturbations (RMPs) have been applied to produce magnetic islands with the intention of driving pedestal gradients below the MHD stability limit. The tearing stability of the resulting non-symmetric equilibria is beyond the scope of this work but it is worth noting that the amplitude of such a RMP driven island depends on the value of Δ' calculated in this work [18].

At first sight, it is perhaps surprising that such high- m calculations cannot always be reduced to a purely local calculation involving only the current gradient and magnetic shear at the rational surface, but instead requires that the complete structure of the q profile be taken into account, albeit in a narrow region for a sharply localised gradient in the current profile. Consideration of this problem is beyond the scope of local gyrokinetic codes. Consequently the extension to a toroidal calculation must inevitably become two-dimensional, unlike problems amenable to the ballooning transformation as in, e.g., the local gyrokinetic code GS2.

Acknowledgments

This work was funded by the RCUK Energy Programme [grant number EP/I501045] and US Department of Energy grant at DE-FG02-91ER-54109 at MIT. IP is supported by the International Postdoc grant of Vetenskapsrådet. To obtain further information on the data and models underlying this paper please contact PublicationsManager@ccfe.ac.uk.

Appendix A. Approximate tearing equation for non-monotonic current profiles

In this appendix A we demonstrate that, using the current distribution of (23) with the parameter $\mu \sim \mathcal{O}(m)$, the global kink/tearing equation (1), can be reduced, in the limit of high- m , to the form of (25) and that, for the case of the $m = 4$ mode investigated in figure 8, the equivalent κ value is 51.1.

We first introduce the notation,

$$p_1 = \frac{\mu}{m}, \quad (\text{A.1})$$

and treat p_1 as $\mathcal{O}(1)$ parameter. Then, in leading order of an expansion in $1/m$,

$$r\hat{J}' = -2p_1 J_1 x, \quad (\text{A.2})$$

now with $x = m(r - r_1)/r_1$. We next construct an expression for $1/q(r) - 1/q(r_1)$ appearing in the denominator of the current drive term of (1), noting that the contributions of the inductive current, $\hat{J}_0(r)$ and the localised current spike, $\hat{J}_1(r)$, are simply additive, so that:

$$\begin{aligned} \frac{1}{q(r)} - \frac{1}{q(r_1)} &= \frac{1}{r^2} \int_{r_1}^r s \, ds [\hat{J}_0(s) + \hat{J}_1(s)] \\ &= \frac{J_0 \hat{r}_1^2 x}{m} \left[-\frac{3}{2} + 2\hat{r}_1^2 - \frac{3}{4}\hat{r}_1^4 \right] + \frac{J_1 x}{m} \left[1 - \frac{p_1 x^2}{3m} \right], \end{aligned} \quad (\text{A.3})$$

where $\hat{r}_1 \equiv r_1/a$. In equation (A.3) we retained an $\mathcal{O}(1/m)$ correction because the leading order term is small at low shear due to near cancellation of the contributions from J_0 and J_1 to $\mathcal{O}(1/m)$. Finally, transforming the radial variable in (1) to x , the kink/tearing equation takes the form,

$$\frac{d^2 \psi}{dx^2} - \psi \left\{ 1 - \frac{2p_1 J_1 x}{mx [J_1 + J_0 \hat{r}_1^2 (-3/2 + 2\hat{r}_1^2 - (3/4)\hat{r}_1^4) - J_1 p_1 x^2 / (3m)]} \right\} = 0, \quad (\text{A.4})$$

which is precisely of the same form as (25) when $x_s = 0$, with the parameter, κ , given by:

$$\kappa = -\frac{2p_1 J_1}{m [J_1 + J_0 \hat{r}_1^2 (-3/2 + 2\hat{r}_1^2 - (3/4)\hat{r}_1^4)]}; \quad (\text{A.5})$$

the above is easily generalised for non zero values of x_s . Note that the above mentioned cancellation of terms in J_0 and J_1 means that κ is formally $\mathcal{O}(1)$ but can become very large and even change sign if the shear at r_1 reverses. For the parameters of figure 7, $J_0 = 2.5$, $J_1 = 1$, $\mu = 64$, $\hat{r}_1 = 0.8$ and for $m = 4$, the equivalent value of κ is 51.1.

References

- [1] Kadomtsev B B and Pogutse O P 1970 *Reviews of Plasma Physics* vol 5, ed M A Leontovich (New York: Consultants Bureau) p 249
- [2] Wesson J A 1978 *Nucl. Fusion* **18** 87
- [3] Strauss H R 1981 *Phys. Fluids* **24** 2004
- [4] Furth H P, Killeen J and Rosenbluth M N 1963 *Phys. Fluids* **6** 459
- [5] Hegna C C and Callen J D 1994 *Phys. Plasmas* **1** 2308
- [6] Pusztai I, Catto P J, Parra F I and Barnes M 2014 *Plasma Phys. Control. Fusion* **56** 035011
- [7] De Bock M F M, Militello F, Huysmans G, Ottaviani M and Porcelli F 2004 *Phys. Plasmas* **11** 125
- [8] Poyé A, Agullo O, Smolyakov A, Benkadda S and Garbet X 2013 *Phys. Plasmas* **20** 020702
- [9] Newcomb W A 1960 *Ann. Phys.* **10** 232
- [10] McCarthy P J and ASDEX Upgrade Team 2012 *Plasma Phys. Control. Fusion* **54** 015010

- [11] De Bock M F M, Citrin J, Saarelma S, Temple D, Conway N J, Kirk A, Meyer H, Michael C A and the MAST Team 2012 *Plasma Phys. Control. Fusion* **54** 025001
- [12] Eriksson H G and Wahlberg C 1997 *Plasma Phys. Control. Fusion* **39** 943
- [13] Barnes M, Parra F I, Lee J P, Belli E A, Nave M F F and White A E 2013 *Phys. Rev. Lett.* **111** 055005
- [14] Drake J F and Lee Y C 1977 *Phys. Fluids* **20** 1341
- [15] Glasser A H, Greene J M and Johnson J L 1975 *Phys. Fluids* **18** 875
- [16] Drake J F, Antonsen T M, Hassam A B and Gladd N T 1983 *Phys. Fluids* **26** 2509
- [17] Cowley S C, Kulsrud R M and Hahm T S 1986 *Phys. Fluids* **29** 3230
- [18] Fitzpatrick R and Hender T C 1991 *Phys. Fluids B* **3** 644